Co-doped Sr_2FeMoO_6 double perovskites: A plausible scenario for phase segregation

H. Chang, M. García-Hernández, M. Retuerto, and J. A. Alonso
Instituto de Ciencia de Materiales de Madrid (CSIC), Cantoblanco, E-28049 Madrid, Spain
(Received 3 December 2005; published 15 March 2006)

The structural, magnetic, and transport properties of Co-doped Sr_2FeMoO_6 in a series of nominal composition $Sr_2Fe_{1-x}Co_xMoO_6$ (x=0, 0.05, 0.1, 0.2, 0.4, 0.7, and 0.9) are studied. At room temperature, the crystal structure is tetragonal with space group *I4/m*. The unit cell and the Fe/Co octahedra volumes increase while the Mo octahedra and Fe/Co-O-Mo bond angles tend to decrease with increasing Co^{2+} content. Antisite disorder clearly decreases along the series and the lattice expands along the *c* direction while contracting in the basal *ab* plane. As expected, it is observed that the ferromagnetic ordering temperature decreases and antiferromagnetic correlations set in with Co doping. Also a spin-glass-like behavior, stemming from the presence of competing ferromagnetic patches in the antiferromagnetic Co^{2+} matrix, is observed for intermediate doping levels. The conductivity exhibits a semiconducting behavior for all samples, although for low Co contents a metallic regime is recovered upon application of an external magnetic field. A maximum in the magnetoresistance is observed for $Sr_2Fe_{0.95}Co_{0.05}MoO_6$ and $Sr_2Fe_{0.9}Co_{0.1}MoO_6$, but surprisingly enough, as an antiferromagnetic and insulating behavior becomes apparent, the heavily doped samples $Sr_2Fe_{0.3}Co_{0.7}MoO_6$ and $Sr_2Fe_{0.1}Co_{0.9}MoO_6$ exhibit magnetoresistive ratios almost the same as those of the corresponding pure compound Sr_2FeMoO_6. The observed phenomenology could be compatible with an electronic phase segregation scenario as has recently been predicted to occur.

DOI: 10.1103/PhysRevB.73.104417 PACS number(s): 75.47.Gk

INTRODUCTION

The Sr_2FeMoO_6 double perovskites have attracted intensive attention due to the large low-field magnetoresistance (MR) exhibited at room temperature.[1,2] Sr_2FeMoO_6 is believed to be a half-metallic material in which conduction electrons are fully spin polarized.[1] The postulated high spin polarization of the carriers at the Fermi level enables spin-dependent scattering processes, and consequently, electronic transport can be strongly influenced by the presence of magnetic fields.[2–5] The ideal structure of Sr_2FeMoO_6 is a stacking of corner-sharing FeO_6 and MoO_6 octahedra, which alternate along the three directions of the crystal, and the Sr cations occupy the voids between the octahedra. The magnetic structure can be viewed as two ferromagnetically (FM) ordered sublattices (Mo and Fe sublattice) antiferromagnetically (AFM) coupled together. However, because of the antisite disorder (ASD), part of the Mo ions occupying the Fe ion site and vice versa, the saturation magnetization is always lower than the predicted value of $4\mu_B$ per formula unit (f.u.). This is due to the AFM correlations existing between two consecutive Fe ions in the antisite disordered material.[6–9] Although ASD reduces the magnetization, it has been shown that moderate levels of antisite disorder benefit the low-field MR.[6,7,10] It has been proposed that antisite-disorder modulates the low-field magnetoresistive response of the system[10,11] and cationic ordering control on the magnetization of Sr_2FeMoO_6 has been widely reported.[7,8] Band structure calculations[12] lead one to think that a significant increase of the Curie temperature T_C could be achieved by electron doping of the parent compound. It was conjectured that the FM coupling between Fe ions in the ideal structure was mediated by the itinerant down-spin electron from Mo and, therefore, an increase of the carriers in the conduction band would increase T_C. Experimentally, this could be realized by substituting the divalent Sr cation by a trivalent cation, typically a rare earth. Indeed, there are plenty of data describing the complete phenomenology of such substitutions.[13,14] Unfortunately, doping of the *A* sublattice greatly influences the antisite disorder, which in turn leads to unwanted side effects in the magnetic and the transport properties of Sr_2FeMoO_6. Recently, a rich phase diagram has been obtained as a function of the separation between the Fe and Mo levels and the band filling.[15] It includes ferri- and antiferromagnetic phases that can be metallic, insulating, or orbitally ordered, and points to the existence of a phase segregation scenario as that depicted for manganites. Also, alternative doping in the *B* sublattice, e.g., the substitution of Mo by W or Re, has been widely studied.[16–23] The latter has been shown to increase the Curie temperature but no improvement of the magnetoresistive properties has been reported.[24]

In regards to the series that we are exploring, results for Sr_2CoMoO_6 have been reported.[25,26] The magnetic moment of Co^{2+} has been found to be about $5.3\mu_B$ due to the extra contribution of the orbital moment,[25] although also a Co^{3+} state has been proposed by Morimoto and co-workers.[27] The existence of an unquenched orbital moment in the *B* sublattice is known to influence the energy levels diagram and therefore it may alter the hybridization scheme, as is the case for the Re-based FeRe and CrRe series. The presence of a non-negligible orbital moment suggests that a plausible strengthening of the FM interaction between Fe ions, leading to an increase of the Curie temperature and to an improvement of the magnetoresitive properties of Sr_2FeMoO_6, could be achieved by doping with a small amount of Co. Also, in contrast to the observation of mixed valence states for the pure conducting FeMo compound $[Fe^{3+}(3d^5)\text{-}Mo^{5+}(4d^1)]$ vs $[Fe^{2+}(3d^6\text{-}Mo^{6+}(4d^0)]$,[28,29] a single $Co^{2+}(3d^7)\text{-}Mo^{6+}(4d^0)$

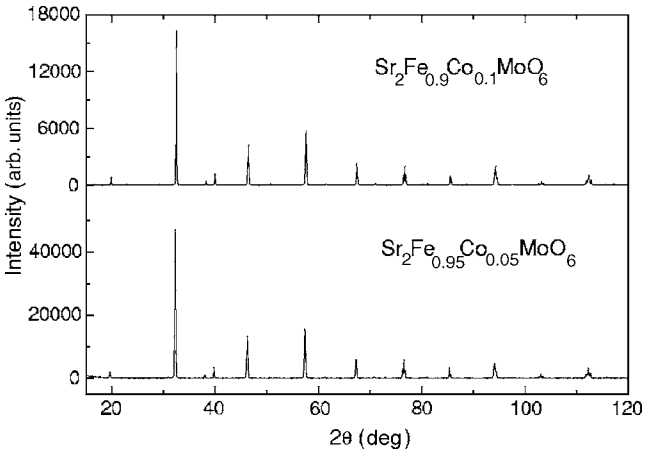

FIG. 1. The Cu $K\alpha$ XRD patterns of $Sr_2Fe_{0.95}Co_{0.05}MoO_6$ and $Sr_2Fe_{0.9}Co_{0.1}MoO_6$.

electronic configuration has been theoretically predicted and experimentaly confirmed for the pure insulating CoMo compound.[25,30] Therefore, as the Co content increases, a gradual transition from a mixed-valence, ferrimagnetic or metallic Sr_2FeMoO_6 to a single-valence, antiferromagnetic or insulating Sr_2CoMoO_6, is expected to occur. In order to shed some light on these hypothesis, we have studied the structural, magnetic, and electronic properties of the Co-doped $Sr_2Fe_{1-x}Co_xMoO_6$ (x=0, 0.05, 0.1, 0.2, 0.4, 0.7, and 0.9).

EXPERIMENTS

The oxygen-stoichiometric $Sr_2Fe_{1-x}Co_xMoO_6$ (x=0, 0.05, 0.1, 0.2, 0.4, 0.7, and 0.9) compounds were prepared by a standard solid state reaction. Stoichiometric mixtures of high-purity $SrCO_3$, $FeC_2O_4 \cdot 2H_2O$, $Mo_7(NH_4)_6O_{24} \cdot 4H_2O$, and $Co(NO_3)_2 \cdot 6H_2O$ were well mixed, ground, and calcined at 900 °C for 24 h in air. After that, the calcined mixtures were reground and reheated at 850 °C in a H_2-N_2 (5-95) reducing flow for 2 h. Finally, the precursor samples were sintered at 1200 °C for 12 h in a flow of H_2-N_2 (2-98). X-ray powder diffraction (XRD) data used for structure refinement were collected at room temperature with Cu $K\alpha$ radiation (40 kV × 30 mA) and a graphite monochromator. A 2θ-scan mode was applied with a step width 2θ=0.04° and a sampling time of 20 s. The step-scanned XRD patterns were fitted using the Rietveld method with the program Fullprof. The magnetization was measured by a commercial superconducting quantum interference device (SQUID) magnetometer. Transport and magnetotransport measurements were performed by the conventional four-probe technique, under magnetic fields up to 8.5 T in a physical properties measurement system (PPMS) from Quantum Design in sintered pellets of $10 \times 3 \times 2$ mm^3.

RESULTS AND DISCUSSION

X-ray diffraction patterns, shown for two represetative samples in Fig. 1, show that all samples $Sr_2Fe_{1-x}Co_xMoO_6$ (x=0, 0.05, 0.1, 0.2, 0.4, 0.7, and 0.9) are single phase double perovskites with group *I4/m*. The lattice parameters, position parameters, and antisite percentages are listed in Table I. It can be seen that the cell volume continuously increases as Co content increases. Both experiments and calculations reveal that the Co ion takes a +2 valence ($3d^7$ configuration) for Sr_2CoMoO_6.[25,26,30] The lattice expansion along the series is consistent with the larger ionic radius of Co^{2+} than that of Fe^{3+}, 0.0885 and 0.0785 nm, respectively. However, from the crystallographic data, we observed that this effect is not isotropic, since the lattice expands along the c direction and contracts in the basal ab plane. The elongation along the c axis has a large influence on the electronic structure since it lifts the threefold degeneracy of Co t_{2g} levels and splits them into a lower-energy doublet (xz/yz) and a higher-energy singlet (xy).[30] The shrinking Mo-O bond length, as shown in Table II, indicates an increasing average valence of the Mo ion, i.e., from +5($3d^1$) to +6($3d^0$) with increasing Co content. This increase in the Mo valence occurrs simultaneously with the gradual change from a mixed-valence state of Fe^{2+}-Fe^{3+} to a single valence state for the Co^{2+}. It is a well-known fact that increasing the ionic radii and charge difference of the atoms in the B sublattice decreases antisite dis-

TABLE I. Crystallographic parameters for $Sr_2Fe_{1-x}Co_xMoO_6$, including the cell and the positional parameters (space group $I4/m$), the antisite proportion, and the discrepancy factors R_{exp}, R_{wp}.

	x						
Parameter	0	0.05	0.1	0.2	0.4	0.7	0.9
a (nm)	0.55740 (3)	0.55738 (2)	0.5.5736 (2)	0.55734 (1)	0.55730 (2)	0.55727 (2)	0.55708 (1)
c (nm)	0.79067 (4)	0.79098 (3)	0.79148 (2)	0.79155 (2)	0.79223 (3)	0.79323 (2)	0.79474 (2)
V (nm^3)	0.245658	0.245734	0.245870	0.245873	0.246054	0.246339	0.246638
4*e* z	0.256 (2)	0.255 (3)	0.257 (2)	0.255 (3)	0.257 (3)	0.257 (2)	0.256 (2)
8*h x*	0.288 (3)	0.287 (3)	0.288 (2)	0.288 (3)	0.288 (3)	0.289 (2)	0.291 (2)
8*h y*	0.225 (2)	0.225 (2)	0.225 (2)	0.225 (2)	0.224 (2)	0.225 (3)	0.225 (1)
Antisite (%)	6.5 (1)	6.8 (1)	6.4 (1)	4.8 (1)	5.9 (1)	2.1 (1)	0.8 (1)
R_{exp}	6.31	4.35	8.81	6.78	6.23	5.98	4.18
R_{wp}	10.15	7.95	13.7	12.5	12.3	10.3	8.1

TABLE II. The interatomic distances (nm) for Fe(Co)-O(×4) and Mo-O(×4) in the basal *ab* plane with four coordination atoms, Fe(Co)-O(×4) and Mo-O(×4) along the *c* direction with two coordination atoms, the average interatomic distance Fe(Co)-O, Mo-O, and Sr-O, and the bond angles (deg) Fe(Co)-O1-Mo and Fe(Co)-O2-Mo.

	x						
Structure	0	0.05	0.1	0.2	0.4	0.7	0.9
				$Fe(Co)O_6$ octahedron			
Fe(Co)-O1(×4)	0.2024	0.2033	0.2039	0.2037	0.2037	0.2043	0.2049
Fe(Co)-O2(×2)	0.2037	0.2021	0.2039	0.2020	0.2038	0.2037	0.2032
⟨Fe(Co)-*O*⟩	0.2027	0.2029	0.2039	0.2031	0.2037	0.2041	0.2043
				MoO_6 octahedron			
Mo-O2(×4)	0.1938	0.1939	0.1919	0.1935	0.1935	0.1930	0.1925
Mo-O1(×2)	0.1930	0.1934	0.1933	0.1938	0.1924	0.1929	0.1942
⟨Mo-O⟩	0.1935	0.1937	0.1924	0.1936	0.1933	0.1930	0.1931
Fe(Co)-O1-Mo	179.99	179.99	179.99	179.99	179.99	179.99	179.99
Fe(Co)-O2-Mo	167.63	166.01	165.05	165.72	165.53	165.34	164.92
				SrO_{12} polyhedron			
Sr-O1(×4)	0.2622	0.2624	0.2617	0.2625	0.2625	0.2624	0.2622
Sr-O2(×4)	0.2972	0.2971	0.2981	0.2972	0.2976	0.2980	0.2987
Sr-O3(×4)	0.2787	0.2787	0.2787	0.2787	0.2787	0.2787	0.2786
⟨Sr-O⟩	0.2794	0.2794	0.2795	0.2796	0.2796	0.2797	0.2798

order. Both the ionic radii and charge differences are larger between Co^{2+} and Mo^{6+} ($Co^{2+} > Fe^{3+} > Mo^{5+} > Mo^{6+}$) as compared to the parent compound (Fe^{3+}, Mo^{5+}), and consequently, increasing the Co^{2+} content tends to decrease the antisite disorder. Indeed, antisite disorder of $Sr_2Fe_{0.1}Co_{0.9}MoO_6$ is only 0.8%, indicating almost absolute ordering within the error range. The depopulation of the conduction band, as inferred from the change of the valence of Mo, aided by the deviation of the bond angle Fe(Co)-O-Mo from 180°, as shown in Table II, work together toward the reinforcement of the insulating state, which is consistent with the observed increase of the resistivity as the Co content increases.

From the magnetic point of view, the saturation magnetization M_s exhibits a non-monotonic behavior, as seen in Fig. 2. Compared with the pure Sr_2FeMoO_6 (SFMO) ($3.83\mu_B$/f.u.), the magnetization of $Sr_2Fe_{0.95}Co_{0.05}MoO_6$ ($3.60\mu_B$/f.u.) decreases, while that of $Sr_2Fe_{0.9}Co_{0.1}MoO_6$ increases ($3.72\mu_B$/f.u.). The intrinsic large magnetic moment of Co^{2+} cations, $5.3\mu_B$/f.u. in pure Sr_2CoMoO_6 also contributes to the variation.[25] The AFM patches Co^{2+}-O-Mo^{6+}-O-Co^{2+} decrease the magnetization, while the isolated Co ions within the ferromagnetic matrix Fe^{3+}-O-Mo^{5+}-O-Fe^{3+} are expected to increase the magnetization. In the low-doping regime, the two double-edged effects are compatible. As more Co ions participate in the structure, the probability of the Co ions forming consecutive AFM chains in the *B* lattice also increases leading to the observed lowering of the total magnetization. A further cross check of the extra contribution of Co to the magnetization comes from the following calculation. If it is assumed that all the Co ions participating in the structure are AFM coupled and the fraction of antisite disorder is *y*, the magnetization *M* is calculated as $M=[M_{Fe}(1-2y)-M_{Mo}(1-2y)](1-x)$ with $M_{Fe}=5\mu_B$ and $M_{Mo}=1\mu_B$. Obviously, without considering the contribution of the FM coupled Co ions, the calculated magnetization should be lower than the experimental value. We find that for the $x=0$ and 0.05 compounds, the calculated magnetization is approximately the same as the experimental value while for the rest of the members of the series, the calculated magnetization is lower than the experimental value, as shown in the inset of Fig. 2. This is consistent with our hypothesis that in all compounds there are some Co ions that remain isolated within the Fe^{3+}-O-Mo^{5+}-O-Fe^{3+} contrib-

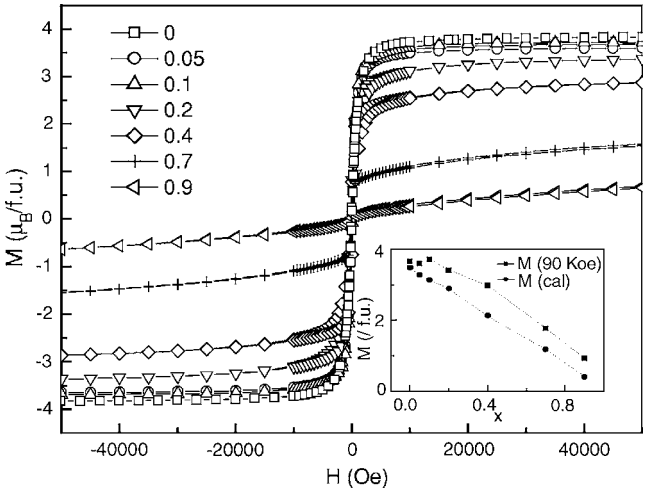

FIG. 2. The magnetization *M* curves of $Sr_2Fe_{1-x}Co_xMoO_6$ ($x=0$, 0.05, 0.1, 0.2, 0.4, 0.7, and 0.9). The inset shows the measured (square) and calculated (circle) magnetization at 50 kOe.

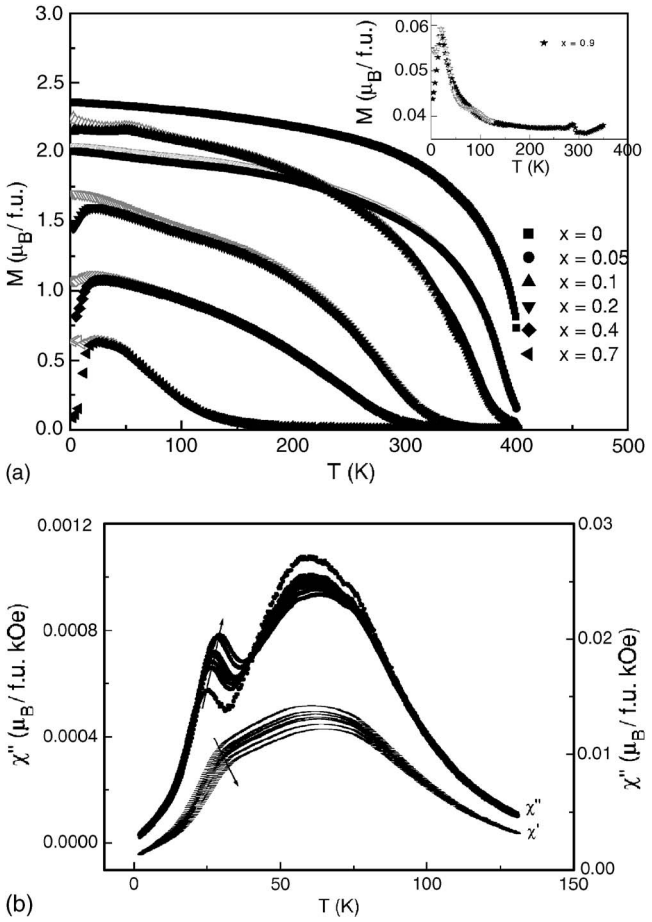

FIG. 3. (a) Magnetization M versus temperature T of $Sr_2Fe_{1-x}Co_xMoO_6$ (x=0, 0.05, 0.1, 0.2, 0.4, and 0.7). The inset shows the ZFC (black solid symbols) and FC (gray hollow symbols) M of $Sr_2Fe_{0.1}Co_{0.9}MoO_6$. (b) The real χ' and imaginary χ'' components of the ac magnetic susceptibility versus T for $Sr_2Fe_{0.3}Co_{0.7}MoO_6$ with the arrow denoting increasing frequency.

uting to the total magnetic moment. Notice that the observed non-monotonic behavior of M_S does not follow the trend of T_C, which systematically decreases as the Co content goes up, as shown in Fig. 3(a). In fact, for $Sr_2Fe_{0.1}Co_{0.9}MoO_6$, the FM is completely suppressed and only a proper Néel temperature at around 22 K can be reported. Therefore we conclude that the strengthening of the FM interactions at very small doping levels, indicated by the enhanced M_S, is limited to a very local scale, in agreement with the postulated existence of isolated Co ions coupled ferromagnetically to the Fe-rich matrix. Along the series what is observed is an overall weakening of the superexchange interaction with Co doping. This can be explained on electronic grounds as the result of the depopulation of the conduction band, although other factors such as the decrease of the bond angle Fe-O-Mo can also contribute. For the pure compound, the Curie temperature is closely related to the number of the electrons in the conduction band near the Fermi level, the carriers mainly provided by Mo^{5+} ions. In the Co-containing Sr_2FeMoO_6, as the doping increases, Mo^{5+} ions are replaced by Mo^{6+}, the density of carries at the Fermi level decreases, since the *pdd* hybridization takes place between the almost unoccupied down-spin Mo t_{2g} orbital and the oxygen orbitals.[30] The pumping out of carriers from the Mo in the conduction band, according to the recent calculations by Taraphder *et al.*,[15] favors a scenario of an electronic phase segregation where a ferromagnetic and metallic nonorbital ordered phase coexists with an antiferromagnetic and insulating orbital-ordered one. An experimental confirmation of the occurrence of such phase segregation could be inferred from the existence of a drastic change in the magnetoresistive properties, resulting from the growth of a conducting phase at the expense of an insulating one when an external magnetic field was applied. Also the existence of a cluster-glass- or spin-glass-like behavior would point out the existence of a favorable scenario for the postulated phase segregation.

A first hint for the latter comes from the increasingly irreversible behavior of the magnetization along the series. For Co content higher than $x \geqslant 0.2$, an irreversible behavior is detected below 30 K, as shown in Fig. 3(a), where zero-field-cooled (ZFC) and field-cooled magnetizations are observed to diverge from each other. In order to ascertain the occurrence of a spin-glass state, we have measured the ac susceptibility of $Sr_2Fe_{0.3}Co_{0.7}MoO_6$, also shown in Fig. 3(b). There are two well-defined peaks, one at about 70 K related to the FM to paramagnetic (PM) transition, and the other at around 30 K which seems to be correlated with the onset of glassy behavior. As expected for a spin-glass system, a clear decrease of temperature for the latter peak is observed as the frequency decreases. The onset of spin-glass behavior is consistent with the plausible coexistence of AFM and FM interactions in the intermediate compounds, which is known to promote strong spin frustration. Besides this magnetic frustration, the disorder in the distribution of the magnetic ions adds another condition that favors the existence of a spin glass. This spin-glass-like behavior strongly influences the macroscopic electrical resistivity as discussed below. For the highest levels of doping in the series, a standard AFM behavior is observed. However, a clear FM contribution is apparent even in $Sr_2Fe_{0.1}Co_{0.9}MoO_6$, as inferred from the hysteretic behavior exhibited in Fig. 2 and a small drop around 290 K in the temperature-dependent magnetization, shown in the inset of Fig. 3(a).

In the Co-poor end of the series, one might conjecture that $Sr_2Fe_{0.95}Co_{0.05}MoO_6$ and $Sr_2Fe_{0.9}Co_{0.1}MoO_6$, are expected to be half-metallic, just like Sr_2FeMoO_6, since, presumably, the density of states should not change very much with Co contents around 5% and 10%. However, the data shown in Fig. 4 reveal that the presence of consecutive Co^{2+}-O-Mo^{6+}-O-Co^{2+} insulating patches spoils the metallic character of the low-doped samples. The insulating behavior of Sr_2CoMoO_6 has been explained by theoretical calculations in terms of the lifting of the t_{2g} triplet degeneracy due to crystal field effects (c-axis elongation of the Co-O bond in the tetragonal structure).[30] This splitting is enhanced by the presence of an on-site Coulomb electronic correlation, giving rise to an insulating gap between the down-spin Co xz/yz doublet and xy singlet. Notice that the metallic character is recovered when an external magnetic field is applied, which in turn renders very high magnetoresistance MR ratios.

Figure 5 shows the measured MR $R(H,T) - R(0,T)/R(0,T)$, at T=5 K for $Sr_2Fe_{1-x}Co_xMoO_6$ (x=0,

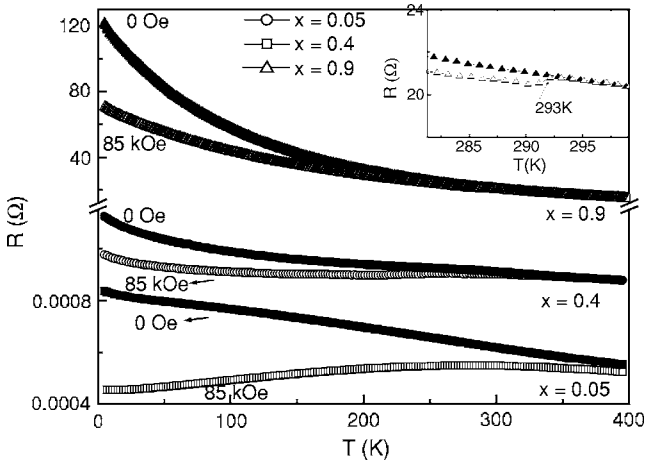

FIG. 4. Resistance R versus temperature T in zero field and 85 kOe for $x=0.05$, 0.4, and 0.9. A zoomed plot of $R(T)$ around 293 K for $x=0.9$ is shown in the inset.

0.05, 0.1, 0.2, 0.4, 0.7, and 0.9). It is found that the low-Co-doped $Sr_2Fe_{1-x}Co_xMoO_6$ ($x=0.05$ and 0.1) samples have larger MR (about −45.8%) than that of the pure compound Sr_2FeMoO_6 (about −42%). Notice also that in these compounds the temperature behavior of the resistivity changes from insulating at zero field to metallic behavior in a high external field. This can be understood as the result of the alignment with the applied field of the highly frustrated spins existing in the proximity of the nanometric Co^{2+}-O-Mo^{6+}-O-Co^{2+} patches. Overcoming this magnetic frustration considerably increases the number of effective good conduction paths and induces a measured MR ratio even larger than that of the pure Sr_2FeMoO_6 compound, for which these AFM interactions are absent (if the samples are perfectly ordered). The slightly larger MR of $Sr_2Fe_{0.9}Co_{0.1}MoO_6$ than that of $Sr_2Fe_{0.95}Co_{0.05}MoO_6$ at 85 kOe is probably related to the slightly larger magnetization of the sample. With the same contour, the magnetoresistive ratios of $Sr_2Fe_{0.8}Co_{0.2}MoO_6$ and $Sr_2Fe_{0.6}Co_{0.4}MoO_6$ are lower than those at $x=0$, 0.05 and 0.1. It is worth mentioning

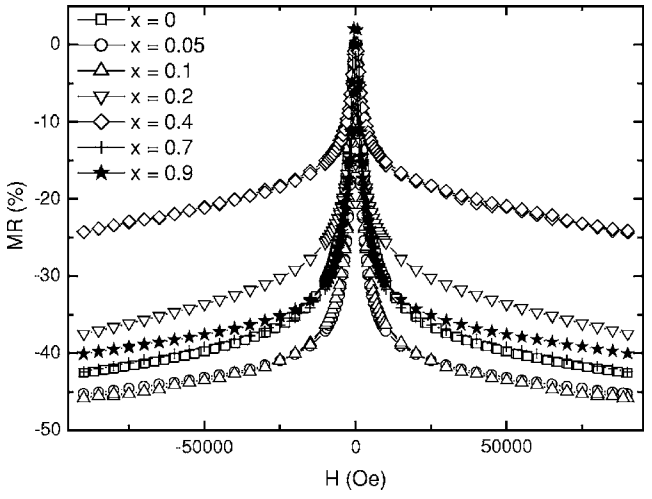

FIG. 5. Magnetoresistance MR of $Sr_2Fe_{1-x}Co_xMoO_6$ ($x=0$, 0.05, 0.1, 0.2, 0.4, 0.7 and 0.9) at 5 K.

that the thermal variations of the low temperature resistances of $Sr_2Fe_{1-x}Co_xMoO_6$, with $x=0.2$ and 0.4, are different from what is observed for the low-doped compounds. This is particularly noticeable when an external field is applied and the metallic behavior in the low doped samples is recovered, as shown in Fig. 4. Notice also that for the $x=0.2$ and 0.4 member of the series, the resistance shows an upturn at low temperature, whose origin can be related to charging effects.[31] In these compounds $Sr_2Fe_{0.8}Co_{0.2}MoO_6$ and $Sr_2Fe_{0.6}Co_{0.4}MoO_6$, the AFM insulating Co^{2+}-O-Mo^{6+}-O-Co^{2+} patches or areas start to percolate. As the Co doping increases, a small fraction of FM Fe^{3+}-O-Mo^{5+}-O-Fe^{3+} regions are distributed in small metallic clusters, in principle not associated with any physical boundary, surrounded by a more insulating matrix (Co-rich regions). Consequently, at low temperature, depending on the effective grain size of the chemical Fe^{3+}-O-Mo^{5+}-O-Fe^{3+} conducting patches, charging effects can take place. This is consistent with the observed reduction in the slope of the low temperature resistance when a field 85 kOe is applied.[32,33]

Interestingly, at the Co-rich end, very large MR ratios are observed for $Sr_2Fe_{0.3}Co_{0.7}MoO_6$ and $Sr_2Fe_{0.1}Co_{0.9}MoO_6$. Although both of them are insulating in zero field and 90 kOe, they exhibit almost the same MR (−40%) as the pure ferromagnetic/metallic compound Sr_2FeMoO_6 (−42%) (see Fig. 4). Since Sr_2CoMoO_6 has no MR at all,[25] it is intriguing to observe such large values of the MR in $Sr_2Fe_{0.1}Co_{0.9}MoO_6$ at 5 K, about −31% at low field 10 kOe and −40% at 90 kOe, as shown in Fig. 5. The large low-field magnetization could be closely related to the intrinsic inhomogeneous (electronic phase segregated) nature of the systems under study, as theoretically predicted. When the average size of the Fe rich ferromagnetic patches decreases to the nanometer scale upon doping, the cluster-glass behavior is reinforced, as pointed out by the increase of the irreversibilities observed in the magnetization. The effect of an applied magnetic field on these highly inhomogeneous and frustrated systems strongly suppresses the spin disorder characteristic of the glassy phase making the ferromagnetic regions grow. When the ferromagnetic phase grows and becomes comparable to the mean free path, the resistance largely decreases in accordance to our observations. Notice also that for $Sr_2Fe_{0.1}Co_{0.9}MoO_6$ the resistance at 90 kOe exhibits a small jump at 293 K, above which the MR totally disappears as shown in the inset of Fig. 4. This jump correlates with a small jump in the magnetization around the same temperature; see the inset of Fig. 3(a). The merging up of the resistance curves corresponding to 0 kOe and 90 kOe is closely related to the melting of the ferromagnetic phase as the temperature increases. Above 293 K, there are no ferromagnetic interactions any more, and the compound is homogeneously PM. The thermal variations of the resistivity of $Sr_2Fe_{0.3}Co_{0.7}MoO_6$ are similar to that of $Sr_2Fe_{0.1}Co_{0.9}MoO_6$. It is insulating, and the resistance at zero field meets that at 90 kOe at a slightly higher temperature of 303 K. The occurrence of CMR coupled to a spin glass state has been previously observed in perovskite related compounds such as $(TbLa)_{2/3}Ca_{1/3}MnO_3$ (Ref. 33) or $RNi_{0.3}Co_{0.7}O_3$.[34] This effect has also been reported for pyrochlorelike compounds such as $Tl_{(2-x)}Bi_xMn_2O_7$.[35]

CONCLUSIONS

We have explored the series $Sr_2Fe_{1-x}Co_xMoO_6$ and fully characterized its structural, magnetic, and transport behavior. For the intermediate members of the series, the Co^{2+} ions form AFM bonds, while the Fe^{3+} ions form FM bonds. The coexistence of FM and AFM bonds produce the spin-glass phase observed for the highly doped samples. Within an electronic phase segregation scenario where metallic FM, insulating AFM regions and highly spin-disordered regions coexist, the inhomogeneous FM mesostructures boost the MR from 0 in Sr_2CoMoO_6 to −40% in $Sr_2Fe_{0.1}Co_{0.9}MoO_6$ at 5 K and 90 kOe. This confirms the recent predictions on the intrinsic inhomogenous nature of these double perovskites.[15] Also, the diluted Co^{2+} ions in $x=0.05$ and 0.1 compounds contribute to the slight enhancement of MR with respect to undoped Sr_2FeMoO_6. It is thought that the application of an external field increases the size of the ferromagnetic domains, hence diminishing the spin fluctuation scattering in the sample.

ACKNOWLEDGMENTS

We acknowledge financial support from the Spanish CICyT (Grants No. MAT2002-01329 and No. MAT2004-00479) and from the CAM government (Grant No. GR/MAT/0771/2004). We are also indebted to F. Guinea for fruitful comments and enlightening conversations. One of us (H.C.) is grateful to the Spanish Ministry of Education for a Mobility Program Grant that enabled her stay at ICMM.

[1] K.-I. Kobayashi, T. Kimura, H. Sawada, K. Terakura, and Y. Tokura, Nature (London) **395**, 677 (1998).
[2] T. H. Kim, M. Uehara, S.-W. Cheong, and S. Lee, Appl. Phys. Lett. **74**, 1737 (1999).
[3] Y. Tomioka, T. Okuda, Y. Okimoto, R. Kumain, and K.-I. Kobayashi, Phys. Rev. B **61**, 422 (2000).
[4] Z. Fang, K. Terakura, and J. Kanamori, Phys. Rev. B **63**, 180407 (2001).
[5] T. T. Fang, Phys. Rev. B **71**, 064401 (2005).
[6] D. Sánchez, J. A. Alonso, M. García-Hernández, M. J. Martínez-Lope, M. T. Casais, and J. L. Martinez, J. Mater. Chem. **13**, 1771 (2003).
[7] LI. Balcells, J. Navarro, M. Bibes, A. Roig, B. Martínez, and J. Fontcuberta, Appl. Phys. Lett. **78**, 781 (2001).
[8] H. Yanagihara, M. B. Salamon, Y. Lyanda-Geller, Sh. Xu, and Y. Moritomo, Phys. Rev. B **64**, 214407 (2001).
[9] D. Sánchez, J. A. Alonso, M. García-Hernández, M. J. Martínez-Lope, and J. L. Martinez, Phys. Rev. B **65**, 104426 (2002).
[10] M. García-Hernández, J. L. Martinez, M. J. Martínez-Lope, M. T. Casais, and J. A. Alonso, Phys. Rev. Lett. **86**, 2443 (2001).
[11] D. D. Sarma, E. V. Sampathkumaran, S. Ray, R. Nagarajan, S. Majumdar, A. Kumar, G. Galini, and T. N. Guru Row, Solid State Commun. **114**, 465 (2000).
[12] D. D. Sarma, P. Mahadevan, T. Saha-Dasgupta, S. Ray, and A. Kumar, Phys. Rev. Lett. **85**, 2549 (2000).
[13] W. R. Branford, S. K. Clowes, Y. V. Bugoslavsky, Y. Miyoshi, L. F. Cohen, A. V. Berenov, J. L. macManus-Driscoll, J. Rager, and S. B. Roy, J. Appl. Phys. **94**, 4714 (2003).
[14] Y. Moritomo, S. Xu, T. Akimoto, A. Machida, N. Hamada, K. Ohoyama, E. Nishibori, M. Takata, and M. Sakata, Phys. Rev. B **62**, 14224 (2000).
[15] A. Taraphder and F. Guinea, Phys. Rev. B **70**, 224438 (2004).
[16] S. Ray, A. Kumar, S. Majumdar, E. V. Sampathkumaran, and D. D. Sarma, J. Phys.: Condens. Matter **13**, 607 (2001).
[17] E. Carvajal, O. Navarro, R. Allub, M. Avignon, and B. Alascio, J. Magn. Magn. Mater. **272-276**, 1774 (2004).
[18] J. Navarro, C. Frontera, L. Balcells, B. Martínez, and J. Fontcuberta, Phys. Rev. B **64**, 092411 (2001).
[19] K. I. Kobayashi, T. Okuda, Y. Tomioka, T. Kimura, and Y. Tokura, J. Magn. Magn. Mater. **218**, 17 (2000).
[20] T. S. Chan, R. S. Liu, G. Y. Guo, S. F. Hu, J. G. Lin, J. M. Chen, and C.-R. Chang, Solid State Commun. **133**, 265 (2005).
[21] X. Zhao, R. C. Yu, Y. Yu, F. Y. Li, Z. X. Liu, G. D. Tang, and C. Q. Jin, Mater. Sci. Eng., B **111**, 101 (2004).
[22] J. J. Blanco, M. Insausti, L. Lezama, J. P. Chapman, I. G. de Muro, and T. Rojo, J. Solid State Chem. **177**, 2749 (2004).
[23] S. Ray, A. Kumar, S. Majumdar, E. V. Sampathkumaran, and D. D. Sarma, J. Phys.: Condens. Matter **13**, 607 (2001).
[24] J. M. De Teresa, D. Serrate, C. Ritter, J. Blasco, M. R. Ibarra, L. Morellon, and W. Tokarz1, Phys. Rev. B **71**, 092408 (2005).
[25] M. C. Viola, M. J. Martínez-Lope, J. A. Alonso, P. Velasco, J. L. Martinez, J. C. Pedregosa, R. E. Carbonio, and M. T. Fernández-Díaz, Chem. Mater. **14**, 812 (2002).
[26] S. A. Ivanov, S.-G. Eriksson, R. Tellgren, H. Rundlöf, and M. Tseggai, Mater. Res. Bull. **40**, 840 (2005).
[27] Y. Moritomo, Sh. Xu, A. Machida, T. Akimoto, E. Nishibori, M. Takata, and M. Sakata, Phys. Rev. B **61**, R7827 (2000).
[28] J. M. Greneche, M. Venkatesan, R. Suryanarayanan, and J. M. D. Coey, Phys. Rev. B **63**, 174403 (2001).
[29] J. Lindén, T. Yamamoto, M. Karppinen, H. Yamauchi, and T. Pietari, Appl. Phys. Lett. **76**, 2925 (2000).
[30] H. Wu, Phys. Rev. B **64**, 125126 (2001).
[31] M. García-Hernández, F. Guinea, A. de Andrés, J. L. Martínez, C. Prieto, and L. Vázquez, Phys. Rev. B **61**, 9549 (2000).
[32] D. Sanchez, M. Garcia-Hernandez, N. Auth, and G. Jakob, J. Appl. Phys. **96**, 2736 (2004).
[33] J. M. De Teresa, C. Ritter, M. R. Ibarra, P. A. Algarabel, J. L. García-Muñoz, J. Blasco, J. García, and C. Marquina, Phys. Rev. B **56**, 3317 (1997).
[34] J. Pérez, J. García, J. Blasco, and J. Stankiewicz, Phys. Rev. Lett. **80**, 2401 (1998).
[35] J. A. Alonso, J. L. Martínez, M. J. Martínez-Lope, M. T. Casais, and M. T. Fernández-Díaz, Phys. Rev. Lett. **82**, 189 (1999).